Engineering and Technology Journal 41 (08) (2023) 1058 - 1067

Engineering and Technology Journal
Journal homepage: https://etj.uotechnology.edu.iq

Image Processing Evaluation of LSP Effect on the Corrosion Rate for the 304 Alloy

Raghad N. Salman*, Razi J.Al-azawi, A. Kadhim

Laser and Optoelectronic Engineering Dept., University of Technology-Iraq, Alsina'a street, 10066 Baghdad, Iraq.
*Corresponding author Email: loe.19.01@grad.uotechnology.edu.iq

HIGHLIGHTS

- The micro-hardness was increased by 49% and the surface roughness by more than ten folds.
- The rate of corrosion was decreased by 93.45% when using laser pulses as corrosion inhibitors with an energy of 920 mJ and pulse repetition of 6 Hz.
- The results were compared with the image processing.

ARTICLE INFO

Handling editor: Evan T. Salim

Keywords:
Laser Shock Processing
Micro Hardness
Surface Roughness
Corrosion Inhibitor
Image Processing

ABSTRACT

The purpose of the study is to inhibit the corrosion rate using the (LSP) laser shock processing technology with an ND-YAG laser utilizing the Q-switched technique with a wavelength of 1046 nm for stainless steel 304 alloy. Laser shock processing (LSP) is a novel surface treatment approach for strengthening metal materials that use a high peak power, a brief pulse, and cold hardening. The laser parameters' effect includes laser pulse energy and pulse repetition rate on the surface properties. The qualities of sample surfaces were investigated, including surface roughness and micro-hardness. The X-ray fluorescence technique was used to analyze the chemical composition of this alloy. The corrosion rate was measured using the polarization method. In particular, pitting corrosion was the option we picked. According to the findings, laser shock processing appears to considerably boost the micro-hardness of the LSP-treated sample. The corrosion causes a decrease in the rate. The result revealed that the corrosion current density was decreased, and the corrosion potential was shifted when the laser pulse energy and the pulse repetition rate were increased. When the laser energy was 920 mj and the pulse repetition rate was 6 Hz, we discovered the lowest rate of corrosion. Digital images are usually achieved by changing continuous signals to digital format. Many factors can affect the quality of an image, such as knowledge requirements, causing noise, low contrast, and badly-defined boundaries, among others. Specifically, we compared the results with those of the image processing.

1. Introduction

Stainless steel is used in cutlery and surgical tools. In particular, stainless steel cooking utensils carry heat well, and they are highly durable, strong, inexpensive, rust resistant when exposed to water or stored without drying, and can be used indefinitely. Specifically, the stainless steel alloy is mostly made up of Fe-Cr-Ni, with minor amounts of Mo, Mn, C, and N. 18-25 wt [1]. Corrosion of metal is the impairment of surfaces and structures caused by a reaction to several elements and conditions. Corrosion in metals is oxidized, and steel is deteriorated [2]. Wet and dry corrosions are the two kinds of corrosion processes classified according to the nature of corrosive surroundings [3,4]. Alloying, coating, anodic protection, cathodic protection, and recently employing the laser for this aim via surface treating of metal are viewed as techniques to improve the qualities of metals, such as roughness, hardness, corrosion resistance, and so on [5, 6]. The process of inhibition of corrosion is essential to reduce the losses caused by corrosion [7,8]. The laser technology made this method very distinguished compared with other sources of energy and made it the traditional technology among all other technologies (even modern ones) used in the heat treatment process. The laser has several special features for surface heating. The first few atomic layers of opaque materials absorb the electromagnetic energy of a laser beam. It was observed that no eddy currents or hot gas jets are associated with the known beam area, and no rays spill out. The applied energy can be accurately directed where needed on the surface; thus, it is described as an actual surface [9-11]. Laser shock peening (LSP) is a technique utilized to change the properties of the metal surface by increasing roughness, hardness, power, and reliability to the material's presence of compressive residual stresses [12,13]. On the other hand, digital image processing is a method that employs computer algorithms for processing digital photographs. Digital image processing provides many advantages compared to analog image processing. In this context, digital images are usually achieved

http://doi.org/10.30684/etj.2023.136032.1294
Received 08 October 2022; Accepted 06 January 2023; Available online 05 February 2023
2412-0758/University of Technology-Iraq, Baghdad, Iraq

by changing continuous signals to a digital format. However, describing the structure by the standard structure analysis can be difficult for any material. In this regard, many factors can influence image quality, including knowledge needs, noise, low contrast, and poorly-defined borders, to name a few. In particular, structure recognition becomes difficult when these components are present in the image. As a result, image processing and digital image collection have become the most important instruments in the characterization of materials in the recent decade. Various images from the microscope and AFM are captured. Image analysis software for computers can be accustomed to analyzing the image. The shape, size, and surface morphology made of microns or nanostructured materials are described via image processing [14]. Considering the above points, this work aims to reduce the resistance of corrosion by increasing the hardness surface of the 304 stainless steel alloy by changing the parameter of the laser, including the pulse energy and the pulse reputation rate.

2. Experimental Methods

2.1 Sample Preparation

The 304 stainless steel was used in this work. Specifically, the samples were cut into circular forms using a turning machine with a diameter of 20 mm and a thickness of 5 mm. Then, the samples were milled using the same roughness grades on SIC papers (800#) to protect the sample's surface from injury and to limit the heat generated by friction between the metal and the papers in the presence of water.

2.2 Chemical Composition Analysis

The chemical content of all samples was determined using the X-ray fluorescence (XRF) technology from Oxford Instruments (Foundry Master Xpert).

2.3 Laser Shock Processing (LSP)

To generate shock waves, a Q-switched Nd-YAG laser with a wavelength of 1064 nm, 30 pulses, and a repetition rate of 2 to 8 was utilized. The laser's energy was increased from 320 m to 920 m. Figure 1 depicts the block diagram.

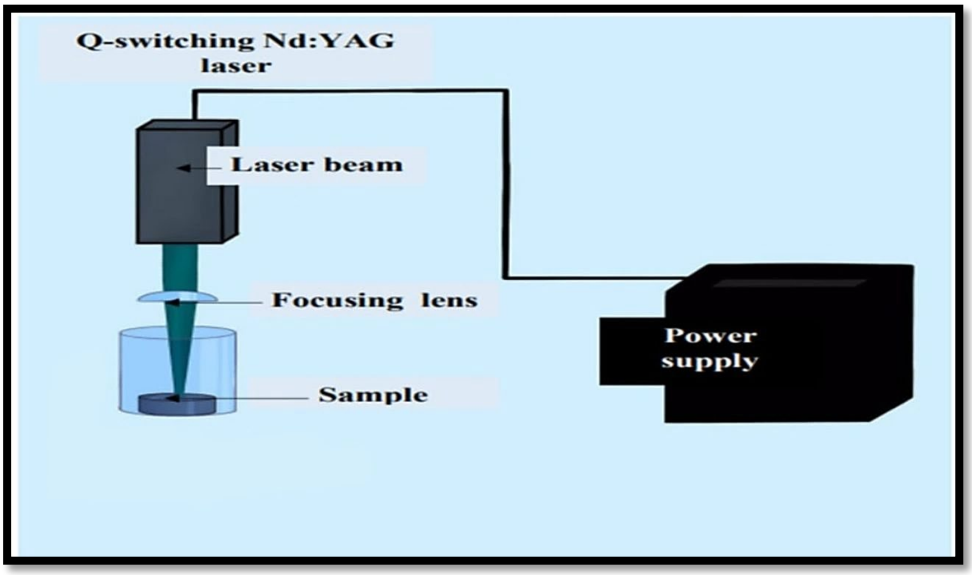

Figure 1: Block diagram of the LSP setup

2.4 Microhardness Test

The microhardness of all samples was determined using a Vickers hardness testing machine (model HVS-1000). The tests were carried out with a 0.981N load for 15 seconds. Before and after the samples were treated, the surface microhardness was assessed. Creating a sufficient microhardness profile in the hardened layer and, as a result, a valid microhardness variation required taking three measurement readings and averaging them to one value. In particular, the microhardness was measured at the laser spot's impact center.

2.5 Surface Roughness Test

All samples were subjected to a surface roughness test. A surface roughness instrument (model TR220) was used within the micro range. Two measurements were obtained and averaged to get the required value.

2.6 Corrosion Test

The corrosion test was used to study the corrosion for all samples of the (304 stainless steel) after the effect of the laser shock penning technique. The preparation of the corrosion solution salty water was accomplished using 17.5 grams of NaCl salt that was added to a half litter of water, as shown in Figure 2.

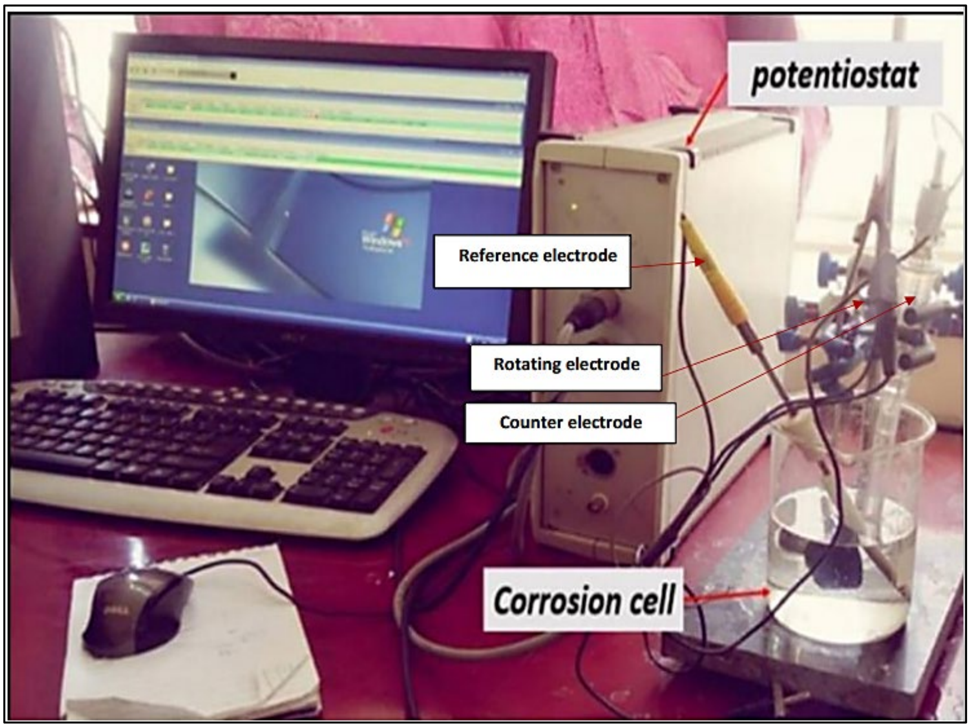

Figure 2: The corrosion cell

2.7 Processing of Images

Images were obtained from the microscope for samples of the (304 stainless steel) before and after the laser treatment. A new material hardness and corrosion evaluation-based digital image processing has been offered using the (Matlab R2018a) program, which was utilized to research image processing methodologies applied on samples before and after laser treatment and system considerations. In this regard, the Program Image J is a java-based image processing application developed by the National Institutes of Health in the United States, and it is built on an open-source architecture that allows for extension and modification using large-scale tools and recorders. In particular, many problems can be solved with written tools.

3. Results and Discussion

3.1 Chemical Composition Result

Table 1 presents the chemical composition of the stainless steel alloy that was used in this work [15].

Table 1: Chemical composition of stainless steel

Sample	C%	Si%	Mn%	P%	S%	Cr%	Mo%	Ni%	Al%	Cu%	Fe%
Shaft	0.06	0.26	1.48	0.029	0.42	17.9	0.58	8.7	0.004	0.43	Bal

3.2 Microhardness Results

The micro-hardness of all materials was measured using the Vickers method before and after the laser shock wave treatment under fixed conditions, including 30 laser pulses and a 6Hz pulse repetition rate. Before the laser shock wave treatment, the average micro-hardness value for the sample was around 181.61 Hv. Figure 3 illustrates the relation between micro-hardness and energy. Specifically, increasing the laser energy from 320 mJ to 920 mJ leads to increasing the micro-hardness from 181.61 Hv to 261.05 Hv. This behavior is due to the finer grain as a result of dislocation strengthening and grain refinement [16].

Figure 4 shows the relation between micro-hardness and pulse repetition rates. In particular, the laser shock wave therapy of pulse repetition rate promotes the micro-hardness, which increased to 217.68 Hv after the laser shock wave treatment. The material intensity of confined plasma peak pressure and propagating shock waves were likewise increased. This trend is consistent with an increase in the compressive residual stress at the material's surface [17].

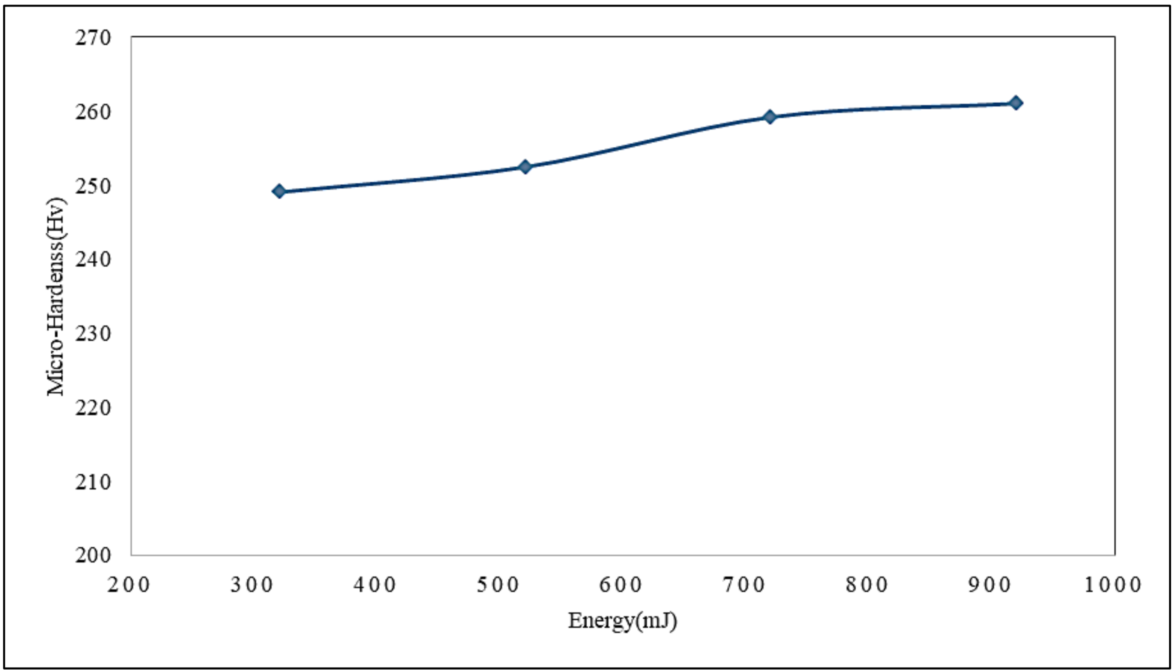

Figure 3: The micro hardness as a function of laser energy at (30 pulses and a 6 Hz pulse repetition rate)

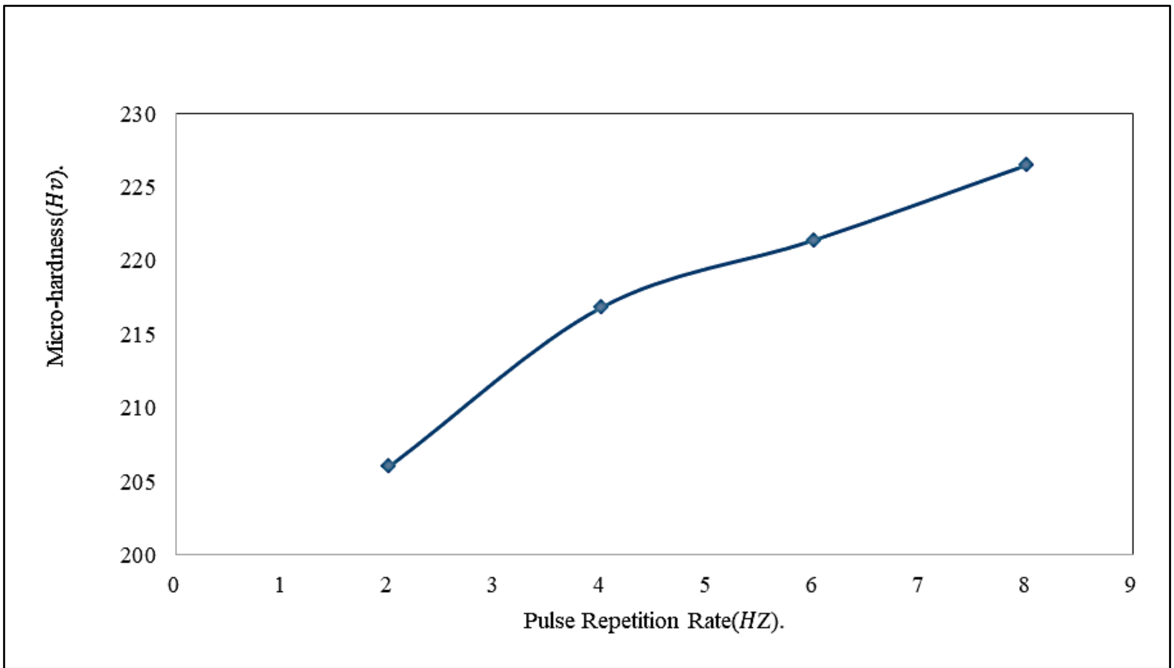

Figure 4: The micro-hardness as a function of pulse repetition rate at (920 mJ of laser energy and 30 pulses)

3.3 Surface Roughness

The surface roughness of all materials was measured using the Vickers method before and after the laser shock wave treatment under fixed conditions, including 30 laser pulses and a 6 Hz pulse repetition rate. The average surface roughness value before the laser shock wave treatment was 0.0505 μm, as shown in Figure 5, which represents the relation between the surface roughness and the energy. Particularly, the roughness slowly increased by changing the pulse energy of the laser until 720 mJ, and the roughness increased remarkably at 920 mJ, where the value of roughness was 0.54. This phenomenon is related to ablation processes connected with the laser shock wave processing at the sample's surface produced by an increase in the laser pulse energy [18].

Figure 6 illustrates the relation between the surface roughness and the pulse repetition rate. In particular, the roughness slowly increased by changing the pulse repetition rate of the laser until 6 HZ, and the roughness remarkably increased at 8 HZ. The nanoparticles at solid targets were expelled with each laser pulse due to the higher pulse repetition rate. Due to the increased pulse repetition rate, nanoparticles at the solid targets were ejected with every laser pulse. This process provides evidence of absorbing sufficient laser energy to guarantee the melting of all defects [19]. In particular, the results show the variation of surface roughness values from (0.057 to 0.969) µm.

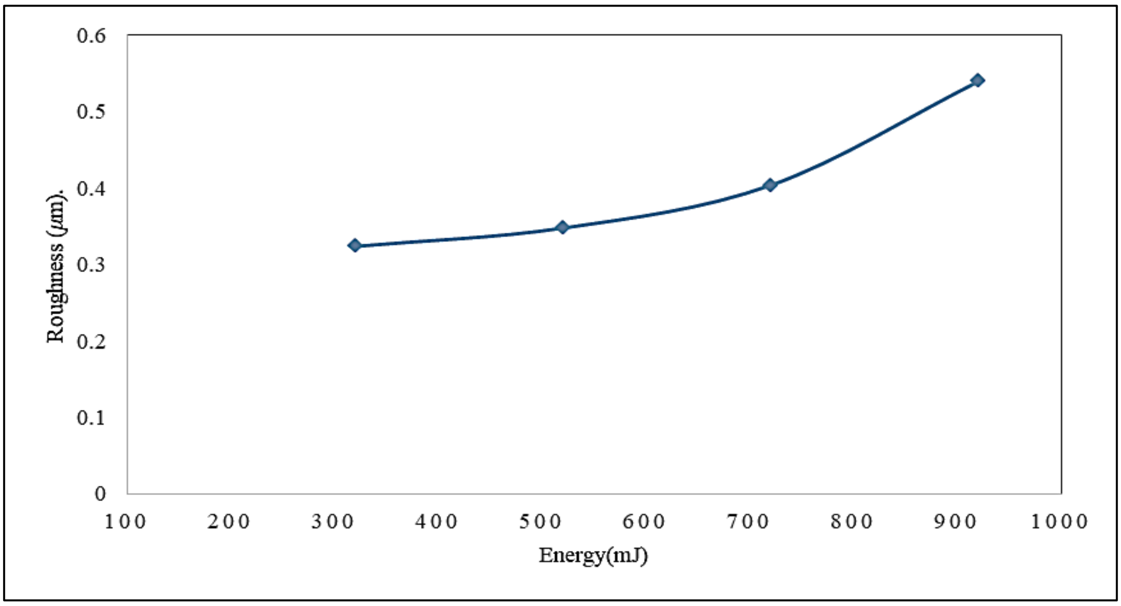

Figure 5: Surface roughness as a function of laser pulse energy at (30 pulses and 6 Hz of pulse repetition rate)

Figure 6: Surface roughness as a function of the pulse repetition rate at (920 mJ of laser pulse energy and 30 pulses)

3.4 Corrosion Rate Inhibition

A polarization approach was used to conduct the corrosion measurements. The corrosion rate was CR= (18.791 mm/y) for samples before the LSP treatment. After the laser treatment under various circumstances, all samples were measured using the same approach. Different LSP parameters were investigated to find the best LSP circumstances and the highest possible laser efficiency to improve the corrosion inhibitor. The energy of the Nd: YAG laser is the first factor studied to see how it affects corrosion resistance. Various energy levels were employed, ranging from 320 to 920 mJ. It is worth noting that the corrosion current density has decreased, and the corrosion potential has shifted [20]. This implies that the contact of the laser with the surface of all samples touching the corrosion solution boosted their corrosion resistance. Before the laser shock processing treatment, the polarization (tafel curve) in Figure 7 shows an increased surface hardness and, consequently, increased corrosion resistance. Figure 8 shows the relationships between the laser pulse energy and the corrosion rate for the samples. The effect of four different laser repetition rates of (2, 4, 6, and 8) on corrosion resistance was tested. As the pulse repetition rate is raised, it can be shown that the corrosion current density drops. As a result, the corrosion rate decreases. Specifically, the corrosion rate is (3.0144mm/yr) at 2 HZ, but the corrosion rate is (2.1785 mm/yr) at 8 HZ, as shown in Figure 9. The build-up heat reaches a larger value. In this regard, the plasma created at high repetition rates is thought to be the source of the heat. Furthermore, plasma remains in liquid for a longer period, and its expansion and contact with the environment are high [21]. Before the laser shock processing treatment, Figure 10 shows that the value of the corrosion rate drops with the pulse repetition rate due to the increased dislocation property caused by the high surface hardening.

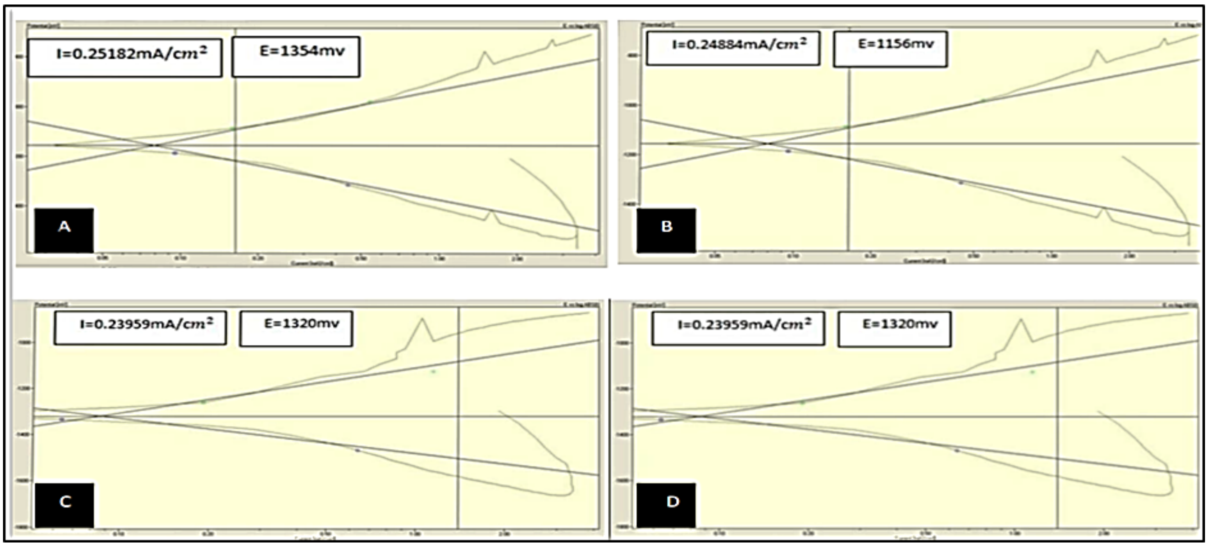

Figure 7: Polarization curve pitting of 304stainless steel alloy after LSP (A:320 mJ, B:520 mJ, C:720 mJ, and D:920 mJ)

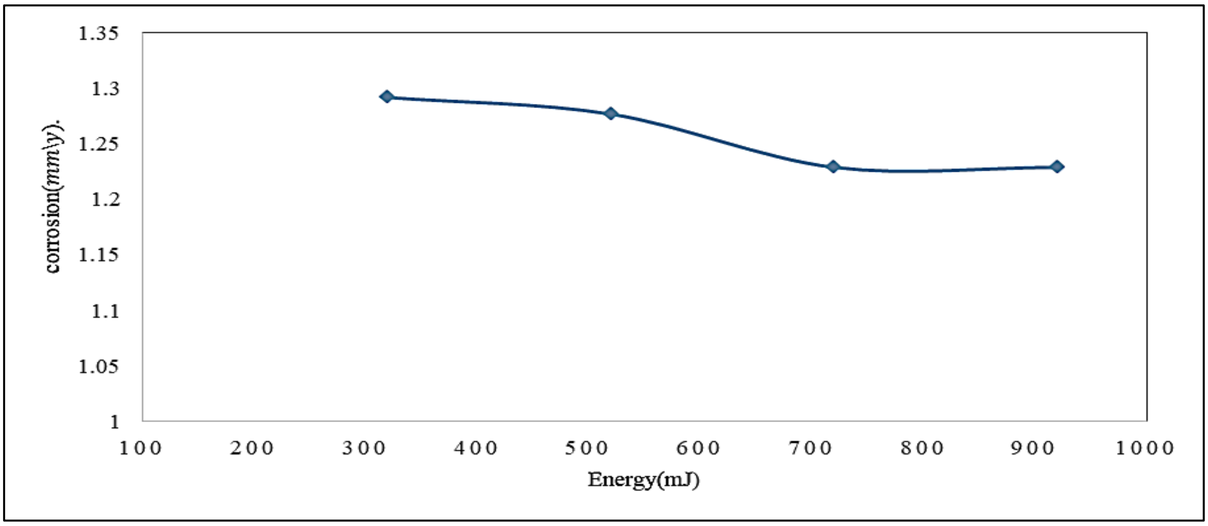

Figure 8: Corrosion rate as a function of laser energy

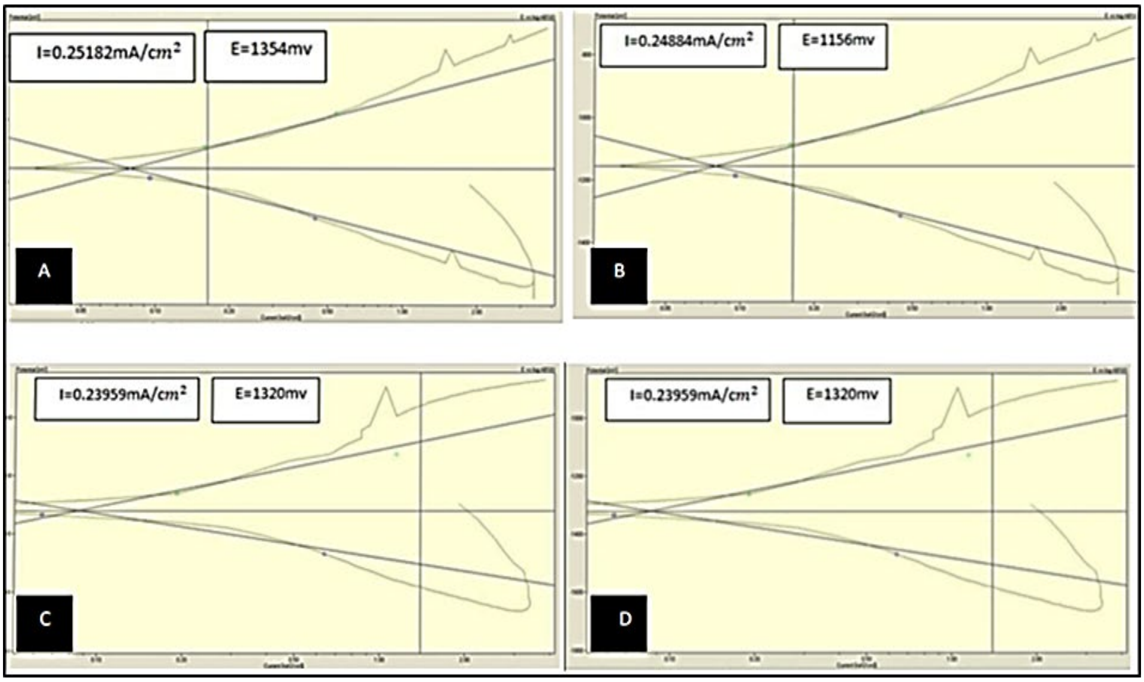

Figure 9: Polarization curve pitting of 304 stainless steel alloy after LSP (A:2, B:4, C:6, and D:8)

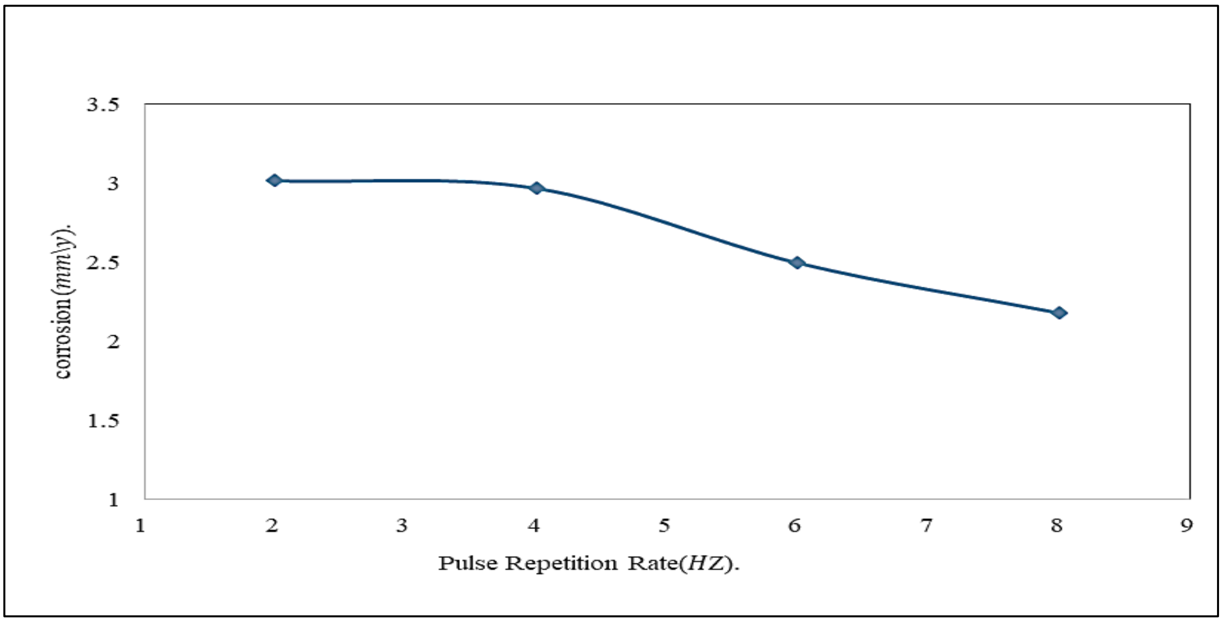

Figure 10: Corrosion rate as a function of pulse the repetition rate for 304 stainless steel alloy pitting type

3.5 Macrostructure

The sheet was cut into circular shapes with a diameter of 20 mm and a thickness of 5 mm to make all the samples. As a result of the grinding machine scratch, the surface is smoother and has fewer pores. Figure 11 shows an optical microscope for a sample that shows the change in the macrostructure after laser and corrosion. Figure 11(a) shows the surface of the sample, which is smooth, before the laser treatment, while Figure 11(b) shows the surface of the sample after the laser treatment showing the spot of the laser. Figure 11(c) shows the surface of the sample after the corrosion showing the pitting on the surface of the sample.

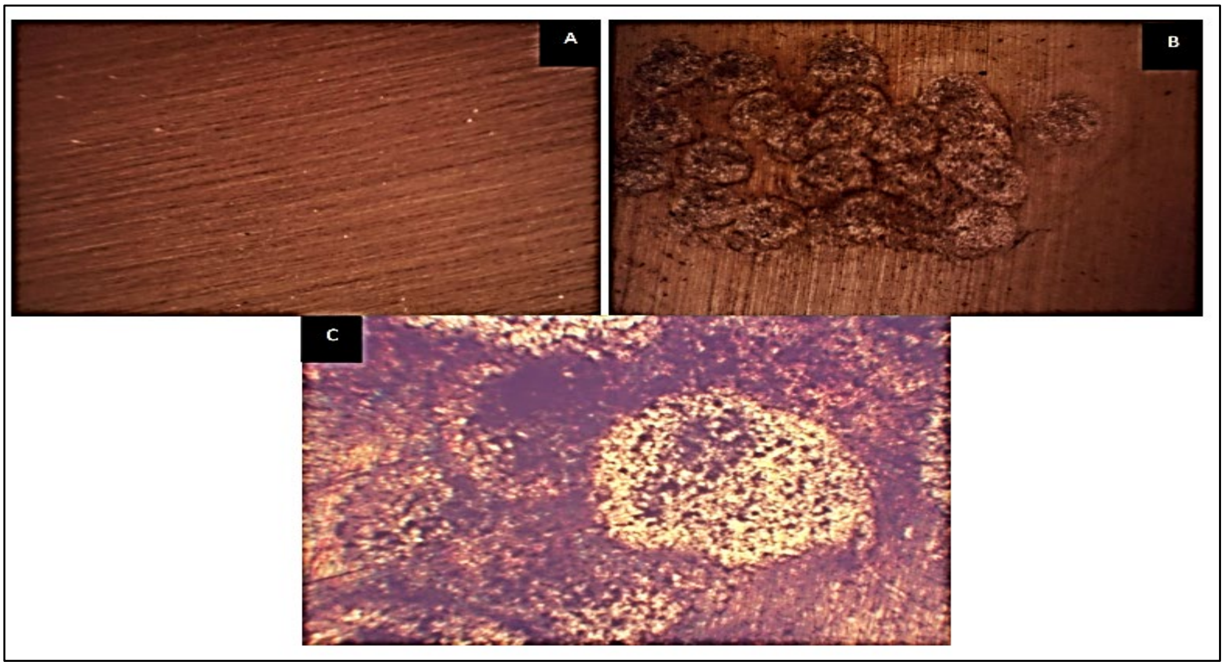

Figure 11: OM image (A: before laser shock wave treatment B: after laser shock wave treatment C: after corrosion)

The results were simulated using MATLAB Rb2018. More specifically, the algorithm has been written in the code of the M-file. The results of the micro-hardness show the effect of various LSP factors on the micro-hardness value for the samples of the 304 stainless steel used in this work following the first effect of the laser energy for the experimental results and the image processing results, as shown in Figure 12. We noticed that the values are almost unchanged. However, we noticed a change in the hardness values at (650 to 920) mJ in actual measurement, while in the image processing-based measurement, we noticed a significant increase in the hardness value between (520 and 920) mJ. The effect of laser repetition is shown in Figure 13 as the relation between hardness and energy. From the comparative study, it is concluded that the results between the practical and the theoretical results are very close.

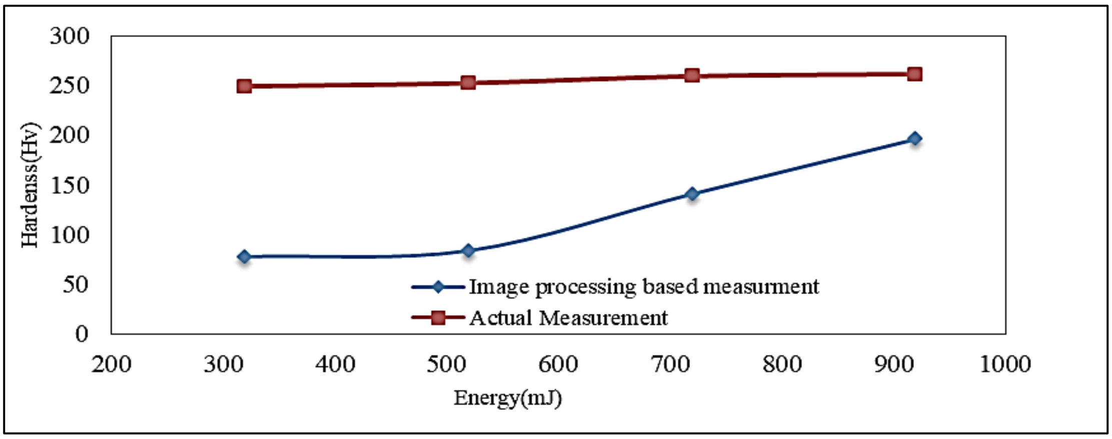

Figure 12: Relationship between actual results and image processing results as a function of laser pulse energy at (30 pulses and 6 Hz of pulse repetition rate)

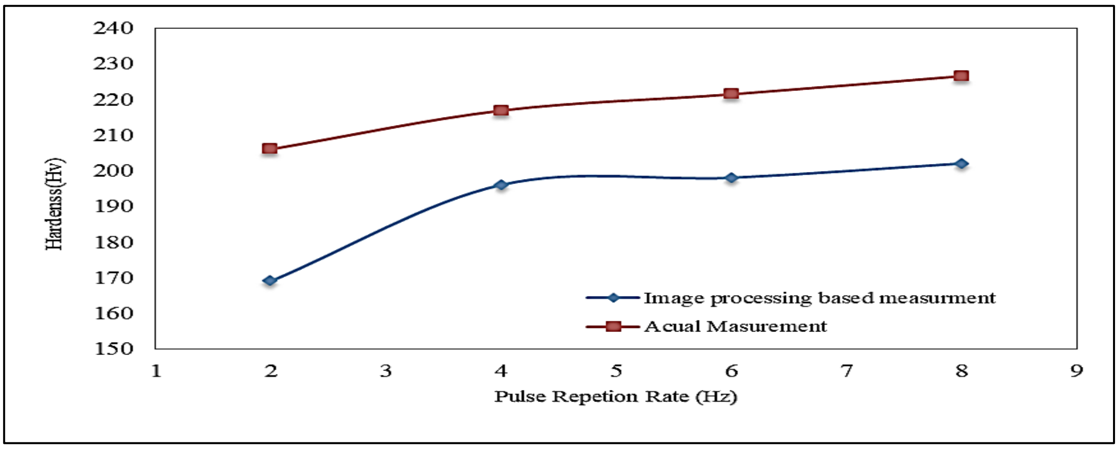

Figure 13: Relationship between actual results and image processing results as a function of pulse repetition rate at (30 pulses and 920 of laser energy)

The results of the corrosion show the effect of various LSP factors on the corrosion value for the samples of the 304 stainless steel used in this work. In particular, for the effect of the laser energy, we note that the rate of corrosion decreases when the energy is increased to 520 mJ, while we note that the rate of corrosion is similar at (520 -720) mJ, but it is lower at 920 mJ. This is shown in the visual part (image processing), while at the actual measurement, approximately an energy of 720 is similar to the value at the energy of 920, as shown in Figure 14 for the experimental results and the image processing as a comparison method. The effect of the pulse repetition rate causes a slight decrease in the value of the corrosion rate at the pulse repetition rate of (2,4) HZ, while it starts decreasing at 6HZ until it reaches its lowest value of 8HZ in actual measurement, while in the image processing, the corrosion rate has the same value approximately at (2,4) HZ, but it began to decrease at 6HZ and approximately 8HZ, as can be shown in Figure 15 that shows the comparison between the results.

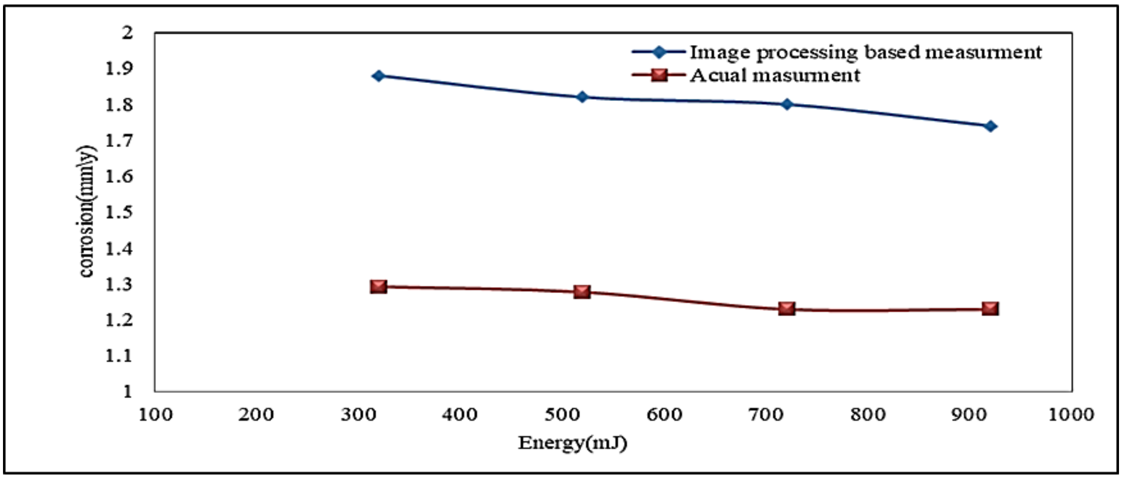

Figure 14: Relationship between actual results and image processing results for the 304 stainless alloy as a function of laser pulse energy at (30 pulses and 6 Hz of pulse repetition rate)

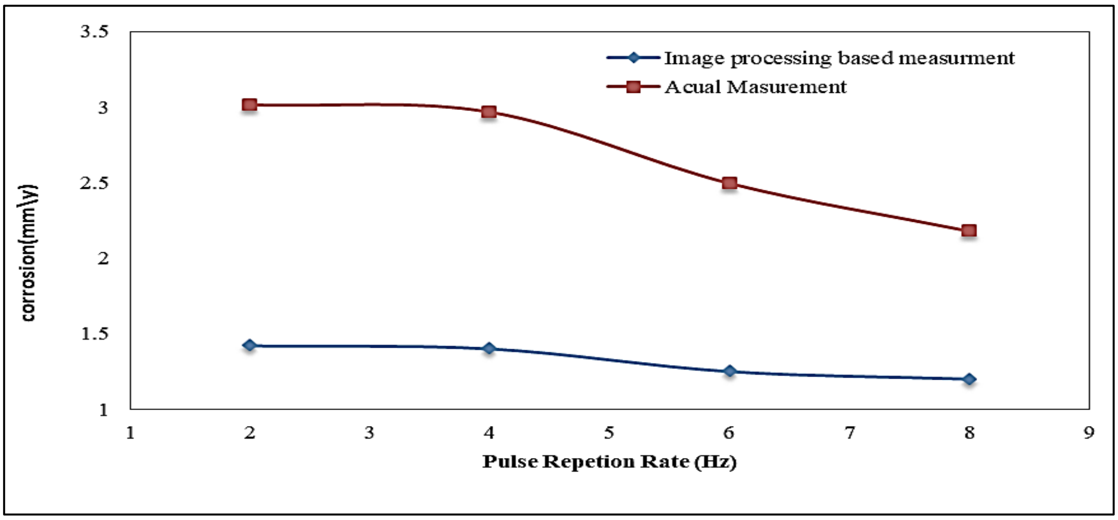

Figure 15: Relationship between actual results and image processing results as a function of laser pulse The energy at (30 pulses and 6 Hz of pulse repetition rate)

4. Conclusion

We conclude from this work that the effect of laser shock processing on the surface properties of the alloy used was clear since the increase of both the laser pulse energy and the repetition rate leads to an increase in both the surface roughness and the micro-hardness. When the laser energy increased from 320 mJ to 920 mJ, the value of the micro-hardness increased by 44%. When the laser pulse repetition rate was increased from 2 to 8 Hz, the micro-hardness values increased by 49%. In addition, increasing the laser energy from 320 to 920 mJ led to a nine-fold increase in surface roughness. Moreover, when the laser pulse repetition rate was changed from 2 to 8, the surface roughness increased more than tenfold. For corrosion inhibition, we chose to pit corrosion and noticed that using LSP leads to increase corrosion inhibition and an increase in corrosion resistance when the laser pulse energy changes or the repetition rate increases. The corrosion rate was decreased by 93.45% when the laser pulses were used as a corrosion inhibitor with an energy of 920mJ and a pulse repetition rate of 6 Hz.

Author contribution

All authors contributed equally to this work.

Funding

This research received no specific grant from any funding agency in the public, commercial, or not-for-profit sectors.

Data availability statement

The data supporting this study’s findings are available on request from the corresponding author.

Conflicts of interest

The authors declare that there is no conflict of interest.

References

[1] F. Padilha, A., R.Rios, P., Decomposition of austenite in austenitic stainless steels , ISI J. Int., 42 (2002) 325-337. https://doi.org/10.2355/isijinternational.42.325

[2] J.R. Davies, Surface Engineering for Corrosion and Wear Resistance, ASM Int., 2001.

[3] G.V. Redkina, A.S. Sergienko and Yu.I. Kuznetsov, Hydrophobic and anticorrosion properties of thin phosphonate–siloxane films formed on a laser textured zinc surface, Int. J. Corros. Scale Inhib., 9 (2020) 1550–1563. http://dx.doi.org/10.17675/2305-6894-2020-9-4-23

[4] A.I. Biryukov, O.A. Kozaderov, R.G. Galin, D.A. Zakharyevich and V.E. Zhivulin, Details of the mechanism of dissolution of iron–zinc coatings based on the δ-phase in acidic media, Int. J. Corros. Scale Inhib., 9 (2020) 1477–1489. http://dx.doi.org/10.17675/2305-6894-2020-9-4-18

[5] A. Kadhim, R.S. Jawad, N.H. Numan and R.J. Al-Azawi, Determination the wear rate by using XRF technique for Kovar alloy under lubricated, Int. J. Comput. Appl. Sci., 2 (2017) 1-5.

[6] M. Hanoon, D.S. Zinad, A.M. Resen and A.A. Al-Amiery, Gravimetrical and surface morphology studies of corrosion inhibition effects of a 4-amino antipyrine derivative on mild steel in a corrosive solution, Int. J. Corros. Scale Inhib., 9 (2020) 953–966. http://dx.doi.org/10.17675/2305-6894-2020-9-3-10

[7] A.A. Al-Amiery, A.A.H. Kadhum, A.B. Mohamad and S. Junaedi, A novel hydrazinecarbothioamide as a potential corrosion inhibitor for mild steel in HCl, Materials, 6 (2013) 1420–1431. https://doi.org/10.3390%2Fma6041420

[8] S. Sathyajith, S. Kalainathan, and S. Swaroop, Laser peening without coating on aluminum alloy Al-6061-T6 using low energy Nd: YAG laser, Opt Laser Technol., 45 (2013) 389-394. https://doi.org/10.1016/j.optlastec.2012.06.019

[9] S. H. Abbas, Effect of hardness on wear resistance of steel. Ph.D. diss., M. Sc. Thesis, University of Technology, 2001.

[10] A. M. Mostafa, M. F. Hameed, and S. S. Obayya, Effect of laser shock peening on the hardness of AL-7075 alloy, J. King Saud Univ. - Sci., 2017. https://doi.org/10.1016/j.jksus.2017.07.012

[11] D.M. Jamil, A.K. Al-Okbi, M.M. Hanon, K.S. Rida, A.F. Alkaim, A. A. Al- Amiery.A.Kadhim, A.A.H Kadhum, Carbethoxythiazole corrosion inhibitor: As an experimentally model and DFT theory, J. Eng. Appl. Sci., 11 (2018) 3952-3959. https://dx.doi.org/10.36478/jeasci.2018.3952.3959

[12] D. A .Mohammed, A.Kadhim, M. A .Fakhri, The enhancement of the corrosion protection of 304 stainless steel using Al_2O_3 films by PLD method. AIP Conf. Proc., 2045(2018) 20014. https://doi.org/10.1063/1.5080827

[13] A. Kadhim, 1 A.A. Al-Amiery, 2 * R. Alazawi, 1 M.K.S. Al-Ghezi2 and R.H. Abass , Corrosion inhibitors. A review. Int. J. Corros. Scale Inhib., 10 (2021) 54–67. http://dx.doi.org/10.17675/2305-6894-2021-10-1-3

[14] H., Peregrina-Barreto, et al. Automatic grain size determination in microstructures using image processing, Measurement. 46 (2013) 249-258. https://doi.org/10.1016/j.measurement.2012.06.012

[15] G. LORANG et al. Chemical composition of passive films on AISI 304 stainless steel, J. Electrochem. Soc., 141 (1994) 3347. https://dx.doi.org/10.1149/1.2059338

[16] K. MUSZKA, J. MAJTA, Ł. BIENIAS, Effect of grain refinement on mechanical properties of microalloyed steels, Metall. Foundry Eng., 32(2006) 87-97. https://doi.org/10.7494/mafe.2006.32.2.87

[17] Z. Wang, Z. Xiaoyan ,H. Weiling , Parameters and surface performance of laser removal of rust layer on A3 steel, Surf. Coat. Technol., 166 (2003) 10-16. https://doi.org/10.1016/S0257-8972(02)00736-3

[18] J. Silcock and G. Willoughby. Proceedings of the Conference on Creep strength in Steel and High-Temperature Alloys, Met.Soc., 2001. 273

[19] J. Kokavec, Z. Wu, J. C. Sherwin, A. J. Ang, and G. S. Ang,. Nd: YAG laser vitreolysis versus pars plana vitrectomy for vitreous floaters, The Cochrane Library (2007). https://doi.org/10.1002/14651858.CD011676.pub2

[20] J. D.Majumdaret al. Effect of laser surface melting on corrosion and wear resistance of a commercial magnesium alloy, Mater. Sci. Eng., A, 361 (2003) 119-129. https://doi.org/10.1016/S0921-5093(03)00519-7

[21] D.A. Mohammed, M. A. Fakhri, A. Kadhim, Reduction The Corrosion Rate Of 304 Stainless Steel Using Pulsed Laser Shock Penning Method, In: IOP Conf. Series: Mater. Sci. Eng., IOP Publishing, 567 (2018) 012162. https://doi.org/10.1088/1757-899X/454/1/012162